

Effect of Pressure on the Fermi Surface of Be†

J. E. SCHIBER AND W. J. O'SULLIVAN

Sandia Laboratories, Albuquerque, New Mexico 87115

(Received 19 February 1969; revised manuscript received 21 April 1969)

Measurements of the effect of hydrostatic pressure on five cross-sectional areas of the Fermi surface of Be are presented. The cross sections were determined from de Haas-van Alphen frequencies obtained with the field-modulation technique. Pressure derivatives were obtained in both solid He to ~ 4 kbar and in fluid He, and results from the two pressure techniques were in excellent agreement in all cases. The most striking result is that for $H\parallel[0001]$ the waist of the third-zone electron surface *decreases* while the hips of this surface *increase*. This behavior cannot be explained even in qualitative terms by free-electron considerations and is at variance with results inferred from recent magnetostriction data. Our results, however, are in substantial agreement with recent calculations by Tripp, Everett, Gordon, and Stark.

I. INTRODUCTION

THE Fermi surface of Be is perhaps the simplest of the hcp group-II metals and consists of only a second-band hole surface known as the "coronet" and two third-band electron surfaces known as "cigars"¹ (see Fig. 1). For fields along symmetry directions, several very prominent sets of de Haas-van Alphen (dHvA) oscillations are observed. For $H\parallel[0001]$, two "cigar" oscillations corresponding to the "waist" and "hips" of the cigar are seen and are denoted α' and α , respectively. For $H\parallel[11\bar{2}0]$ and $H\parallel[10\bar{1}0]$, the spin splitting term $\cos(\pi gm^*/2m_0)$ enhances the second harmonic compared to the fundamental of the cigar oscillations, because m^*/m_0 is nearly $\frac{1}{2}$. Therefore, the second harmonic of the dHvA frequency is most easily seen for this orientation.¹ For $H\parallel[11\bar{2}0]$, oscillations which are due to orbits about the minimum cross sections of the coronet waists are detected, and the corresponding dHvA frequency is labeled γ . A maximum extremal cross section for a $(11\bar{2}0)$ plane through the hole surface near the edges of the Brillouin zone gives rise to what are known as the β_1 oscillations. A similar cross section for $H\parallel[10\bar{1}0]$ gives rise to the β_2 oscillations. Recently, experimental values accurate to about $\pm 0.3\%$ have been obtained for these cross sections, and these values have been fitted to within 1% by means of a nonlocal pseudopotential model.²

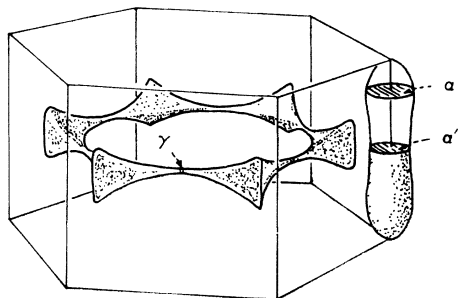


FIG. 1. Fermi surface of Be. We are indebted to M. H. Halloran for this figure.

In this paper we present pressure derivatives for several cross-sectional areas of the Fermi surface of Be. Such data can provide rather critical tests for the physical significance of models describing the Fermi surface of a metal. For example, a local pseudopotential model used by Anderson and Gold³ to describe Pb could *not* account for the pressure derivatives of the cross-sectional areas.⁴ It has been shown that a non-local model potential of the Heine-Abarenkov form is consistent with both the normal-volume and the pressure-dependent dHvA data.⁵ Tripp *et al.*² have indicated that they are testing their model with respect to both alloying⁶ and lattice strain.⁷ Since alloying invariably changes the lattice spacing, data such as those presented in this paper are required for both comparisons.

Recently, Tripp, Everett, Gordon, and Stark⁷ calculated the pressure dependence of Be using the non-local pseudopotential model discussed in Ref. 2. We can compare directly with their results for pressure derivatives of several cross sections.

The effect of stress on cross-sectional areas of the Fermi surface can be obtained from the oscillatory magnetostriction.⁸ Such data for Be have been obtained by Chandrasekhar, Fawcett, Sparlin, and White,⁹ so that we can also compare our results¹⁰ with those of this technique.

In Sec. II we discuss in some detail our experimental procedure. The results are presented and discussed in Sec. III. Section IV consists of a brief summary of our conclusions.

³ J. R. Anderson and A. V. Gold, Phys. Rev. **139**, A1459 (1965).

⁴ J. R. Anderson, W. J. O'Sullivan, and J. E. Schirber, Phys. Rev. **153**, 721 (1967).

⁵ J. R. Anderson, W. J. O'Sullivan, and J. E. Schirber (to be published).

⁶ J. H. Tripp, P. M. Everett, W. L. Gordon, and R. W. Stark (to be published).

⁷ J. H. Tripp, P. M. Everett, W. L. Gordon, and R. W. Stark, Phys. Rev. **180**, 669 (1969).

⁸ B. S. Chandrasekhar, Phys. Letters **6**, 27 (1963).

⁹ B. S. Chandrasekhar, E. Fawcett, D. M. Sparlin, and G. K. White, in *Proceedings of the Tenth International Conference on Low Temperature Physics, Moscow, 1966*, edited by M. P. Malkov (Proizvodstvenno-Izdutclsk'ii, VINITI, Moscow, 1967).

¹⁰ W. J. O'Sullivan and J. E. Schirber, Phys. Letters **25A**, 124 (1967).

* Work supported by the U. S. Atomic Energy Commission.

¹ B. R. Watts, Proc. Roy. Soc. (London) **A282**, 521 (1964).

² J. H. Tripp, W. L. Gordon, P. M. Everett, and R. W. Stark, Phys. Letters **26A**, 98 (1967); P. M. Everett, W. L. Gordon, and R. W. Stark (to be published).

II. EXPERIMENTAL TECHNIQUES

The samples used in this study were cut from distilled, zone-refined material prepared by Nuclear Metals, Inc. The first sample S120, was a right circular cylinder $\frac{1}{8}$ in. diam by $\frac{1}{8}$ in. long, with the cylinder axis parallel to [0001]. The second crystal, S116, was in the shape of a parallelepiped about $\frac{3}{8}$ in. long and $\frac{1}{16} \times \frac{1}{16}$ in. in cross section, with the [1120] axis parallel to the long dimension. These two samples were loaned to us by W. L. Gordon of Case-Western Reserve. The third crystal, S174, was in the shape of a segment cut from a $\frac{1}{8}$ -in.-thick, $\frac{1}{2}$ -in.-diam disk with the long dimension along [0001]. This sample was kindly provided by G. London of the Franklin Institute. The samples had nominal residual resistance ratios of the order of 10^3 .

Hydrostatic pressures to 4 kbar were generated by careful isobaric freezing of He about the samples.¹¹ The fluid-He phase-shift method¹² for pressures^{13,14} below the freezing curve (~ 1800 lb/in.² at 4°K, ~ 380 lb/in.² near 1°K) was also used. All measurements reported were obtained in the 1–4°K temperature range.

The dHvA oscillations were detected using the low-frequency field-modulation technique.^{12,15,16} Since a variety of experimental conditions was utilized to optimize the signal, these conditions will be discussed briefly below with respect to the corresponding cross-sectional areas. (For a more detailed description of our apparatus, see Refs. 4 and 14.)

A. Hole Surface

Data for the second-zone hole surface were taken only for fields along [1120] using sample S116. Since the frequency² associated with the minimum cross-sectional area of the hole coronet surface is 1.09×10^6 G, the optimum field range for observation of the cross section is below 5 kOe. Locked-in flux makes our 55-kOe superconducting solenoid difficult to use in this field range, so data were taken in a nitrogen-cooled compensated Cu solenoid over a field range of 0.7–1.1 kOe, using solid-He pressure generation to 4 kbar. Phase shift measurements were also taken at 1.1°K and 0.8 kOe in this solenoid using the relation

$$(1/B)\Delta H/\Delta P = d \ln F/dP, \quad (1)$$

where B is the field at which the data were taken, ΔH is the applied field necessary to return the oscillation to its position before the increment of pressure ΔP

¹¹ J. E. Schirber, in *Physics of Solids at High Pressures*, edited by C. T. Tomizuka and R. F. Emrick (Academic Press Inc., New York, 1965).

¹² D. Shoenberg and P. J. Stiles, Proc. Roy. Soc. (London) **A281**, 62 (1964).

¹³ I. M. Templeton, Proc. Roy. Soc. (London) **A292**, 413 (1966).

¹⁴ W. J. O'Sullivan and J. E. Schirber, Phys. Rev. **170**, 667 (1968).

¹⁵ A. Goldstein, S. J. Williamson, and S. Foner, Rev. Sci. Instr. **36**, 1356 (1965).

¹⁶ R. W. Stark and L. R. Windmiller, Cryogenics **8**, 272 (1968).

was applied, and $d \ln F/dP$ is the logarithmic pressure derivative of the dHvA frequency.

The dHvA frequency² due to the maximum extremal cross-sectional area of the coronet hole surface for $H \parallel [1120]$ (β_1) is 1.24×10^7 G. This frequency competes with the fundamental and particularly with the second harmonic of the frequency due to the long section of the third-zone electron "cigar." Since the mass associated with the β_1 frequency is about 0.26 compared with ~ 0.5 and ~ 1.0 for the fundamental and second harmonic cigar frequencies, it is of considerable advantage to make measurements at 4°K. Further discrimination is achieved by setting the Bessel function $J_n(x)$ near a zero of the second dHvA harmonic of the cigar frequency. Here, n is the harmonic of the modulation frequency detected, and $x = 2\pi F H_{\text{mod}}/B^2$. F is the dHvA frequency, H_{mod} is the peak modulation amplitude, and B is the dc magnetic field. Proper choice for x can put the ratios of the amplitudes of the coronet necks, the β_1 , and second dHvA harmonic cigar frequencies at $10^{-8}:1:10^{-3}$ for fourth harmonic detection of the 100-Hz modulation frequency. Data were therefore obtained at 4°K at several fields near 20 kOe using fluid-He pressures to 1800 lb/in.²

B. Electron Surface

As mentioned above, the fundamental of the cigar frequency for $H \parallel [1120]$ is difficult to observe, so pressure data were obtained on the second dHvA harmonic only. Since these data were obtained using the phase-shift technique, this was advantageous since the index of the oscillation investigated (or, correspondingly, the value of F with respect to B) was a factor of 2 larger at a given field. To prevent, as much as possible, interference from the β_1 oscillations, data were taken at the 12th harmonic of the 100-Hz modulation frequency at the optimum modulation amplitude. This results in a Bessel-function contribution ratio of $10^{-8}:10^{-2}:1$ for β_1 , a fundamental dHvA cigar, and second dHvA harmonic cigar frequencies, respectively. Data were taken in the range 35–55 kOe at 1.1°K.

For $H \parallel [0001]$, the oscillations due to two cigar cross sections interfere as shown in Fig. 2. For reasons that will become apparent in the discussion, the pressure derivatives of these two cross sections were carefully determined in three different ways.

Method 1. The first method consisted of measuring the carrier frequency α and the number of cycles per beat

$$n = \frac{\alpha}{\alpha - \alpha'} \quad (2)$$

at zero pressure and 4 kbar using sample S120. Differentiation of Eq. (2) with respect to pressure gives

$$\frac{d \ln n}{dP} = \frac{\alpha}{\alpha - \alpha'} \left(\frac{d \ln \alpha'}{dP} - \frac{d \ln \alpha}{dP} \right). \quad (3)$$

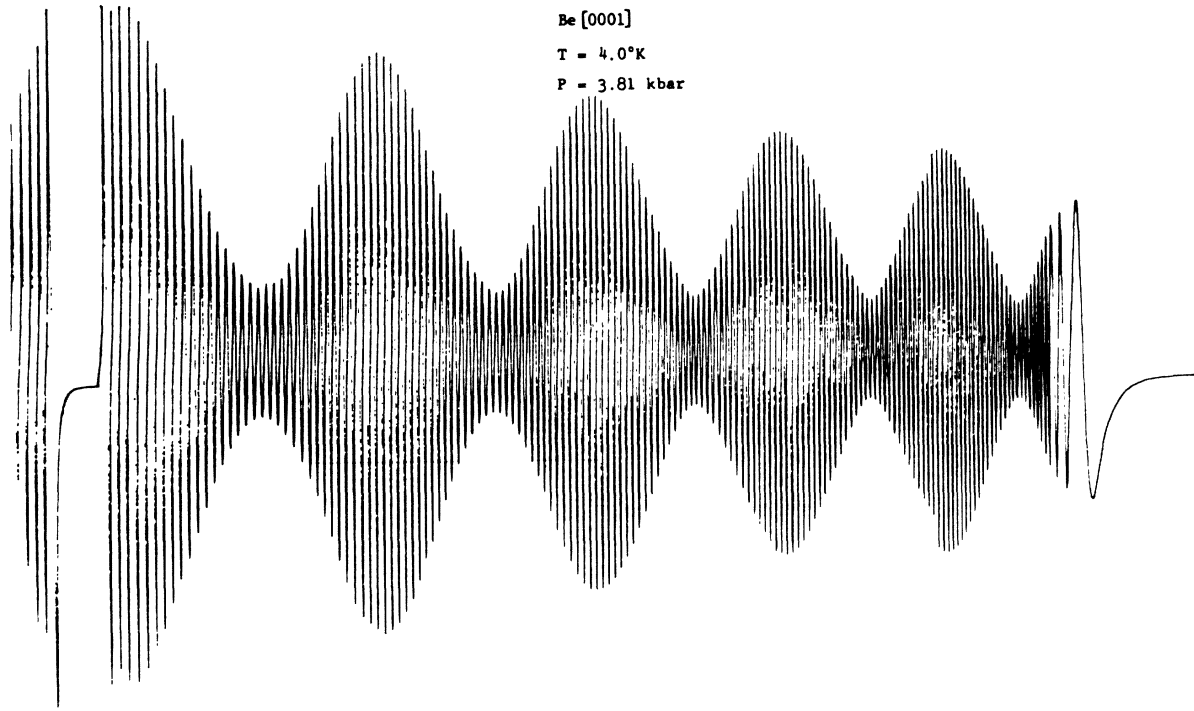


FIG. 2. Reproduction of the third-zone electron (cigar) oscillations in the magnetization for $H \parallel [0001]$.

Since the total change in the carrier frequency is of the order of 0.1% for this pressure interval, care was taken to measure over an integral number of beats (as many as 20). For the modulation amplitude used, the signal corresponds closely to the second derivative of a sawtooth pattern, particularly at 1°K. By carefully adjusting the field to the top of the sharp spike in the pattern, an integral number (to 0.02 or better) of oscillations could be counted. Combining the pressure derivative of the carrier frequency (in this case α) with Eq. (3) yields the pressure derivative of α' .

Method 2. The second method consisted in phase shifting the individual oscillations in the node and antinode of the beat pattern. The relation between these shifts and the logarithmic derivatives of the two frequencies involved is given by

$$\frac{1}{B} \frac{\Delta H^\pm}{\Delta P} \equiv \delta^\pm = \frac{d \ln \alpha}{dP} + \left(\frac{d \ln \alpha'}{dP} - \frac{d \ln \alpha}{dP} \right) (1 \pm R)^{-1}, \quad (4)$$

where $R = A(\alpha)\alpha/A(\alpha')\alpha'$, $A(\alpha)$ is the peak amplitude of the α frequency, and the plus and minus refer to the antinode and node positions in the beat pattern, respectively. As shown previously,¹⁴ this equation holds for a single harmonic pattern whether or not the B - H effect is operative. Figures 3 and 4 show data taken at 4°K near 10 kOe in the node and antinode portions of the pattern. This technique was employed on samples S120 and S174 in solenoids, and on S116 in a transverse field. Results were consistent, but data from S120 are considered to be most accurate.

From method 1, $d \ln \alpha / dP$ was found to be negative, so it follows from Eq. (3) that $d \ln \alpha / dP - d \ln \alpha' / dP > 0$. This same inequality follows directly from the results of method 2 in that the shift in the node of the pattern (α dominant) is greater than that in the antinode in the positive sense as seen in Figs. 3 and 4. Defining $d \ln \alpha / dP - d \ln \alpha' / dP \equiv \Delta$, we can rewrite Eq. (4) as

α dominant:

$$\delta^+ = \frac{d \ln \alpha}{dP} - \frac{\Delta}{R+1}, \quad \delta^- = \frac{d \ln \alpha}{dP} + \frac{\Delta}{R-1}, \quad (5)$$

α' dominant:

$$\delta^+ = \frac{d \ln \alpha'}{dP} + \frac{\Delta}{R+1}, \quad \delta^- = \frac{d \ln \alpha'}{dP} - \frac{\Delta}{R-1}. \quad (6)$$

We observed that the shift at the antinode δ^+ was always positive (see Fig. 4) for α dominant, and since Δ is positive, it follows from Eq. (5) that $d \ln \alpha / dP$ is positive. The direct measurement of α (method 1) as a function of pressure to 4 kbar also gives this result. Thus, methods 1 and 2 give essentially the same information, i.e., $\Delta > 0$ and $d \ln \alpha / dP > 0$. These results are well outside experimental uncertainty. From either of the two methods, the value of $d \ln \alpha' / dP$ can be obtained with somewhat greater uncertainty due to propagation of the errors of two measurements. Although the values obtained by the two methods agree within estimates of the experimental uncertainty, it was important, as discussed in the following section,

to show that the two cross sections have opposite pressure derivatives. Therefore, a third method was devised to show specifically the signs of the two derivatives.

Method 3. Conclusive measurements of the sign of the two pressure derivatives were obtained by adjusting the Bessel-function argument such that only one of the cross sections contributed to the dHvA signal. Phase-shift measurements at 4°K were then taken on sample S174. Data were taken at the antinode position, since by examination of Eqs. (5) and (6) it is evident that if R is close to unity, the term involving Δ can dominate the sign of δ^- . This was not the case for the actual measurements, since it was possible to set the modulation amplitude so that the ratio of the two dHvA amplitudes was of the order of 20 or more. Since the two frequencies differ by only 3%, the amplitude of the retained frequency was seriously diminished. At this diminished amplitude, the second harmonic and/or sum frequency $\alpha+\alpha'$ could be substantial. It was, therefore, advantageous to pick a modulation value such that both α (or α') and $\alpha+\alpha'$ and 2α were near Bessel-function zeros. Thus data were taken at the sixth harmonic of the modulation frequency near the $x=13.59$ zero at 12.655 kOe and 4°K. Figure 5 shows the results of time averaging (by means of a 1024-channel time-averaging computer) for 5 and 10 sweeps of the α and α' frequencies, respectively. Each set of three tracings consists of pressure, zero pressure, and pressure traces plotted from top to bottom over the same field scan and taken in that sequence. Careful examination of these patterns reveals that the outer

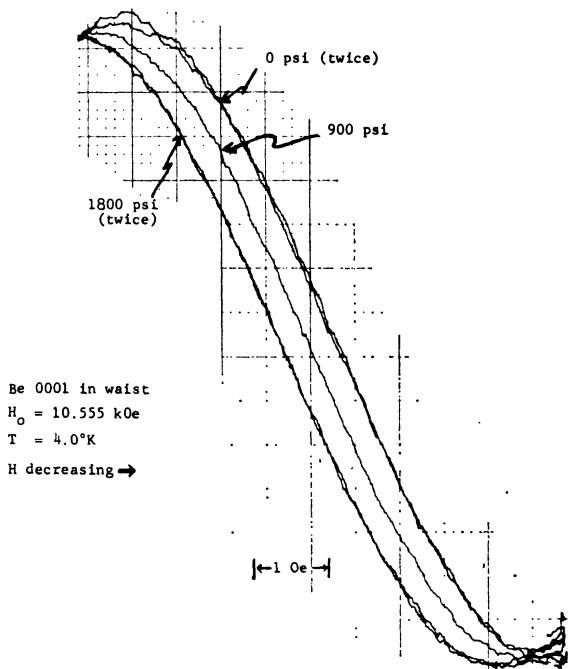


FIG. 3. Reproduction of fluid-He phase-shift data in the node of the cigar beat pattern for $H||[0001]$.

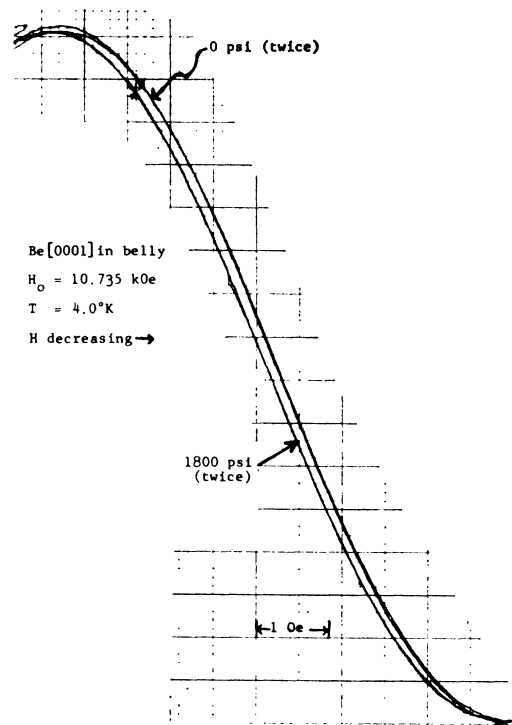


FIG. 4. Reproduction of fluid-He phase-shift data in the antinode of the cigar beat pattern for $H||[0001]$.

curves are shifted to the right or towards lower field for the upper set of α' or waist patterns and to the left for the lower set of α or hip patterns. Since the shift in field is opposite, the pressure derivatives [by Eq. (1)] are of opposite sign. The change in phase results from the change in sign of the Bessel function in going from the null of the α frequency to the null of the α' .

III. RESULTS AND DISCUSSION

The results for the pressure derivatives for the hole surface cross sections are given in Table I. The coronet waists decrease at a rate of $-4.5(\pm 1.0) \times 10^{-3}$ kbar $^{-1}$. This value is the mean of the solid-He and fluid-He results which agree within experimental uncertainty. The pressure derivative of the coronet belly frequency β_1 is $3(\pm 1) \times 10^{-4}$ kbar $^{-1}$. This result was obtained only in fluid He.

The results for the pressure derivatives of the electron surface cross sections are summarized in Table II. For $H||[0001]$, the cigar hip cross section α increases

TABLE I. Summary of pressure derivatives obtained for cross sections of the second-band hole surface (coronet) of Be. The dHvA frequencies quoted are from Ref. 2.

Cross section	Frequency	Field direction	$d \ln F / dP$ (in kbar $^{-1}$)	Pressure technique
Coronet waist (γ)	1.09×10^6	$[11\bar{2}0]$	$-5(\pm 1) \times 10^{-3}$	solid He
			$-4(\pm 1) \times 10^{-3}$	fluid He
Coronet belly (β_1)	1.24×10^7	$[11\bar{2}0]$	$3(\pm 1) \times 10^{-4}$	fluid He

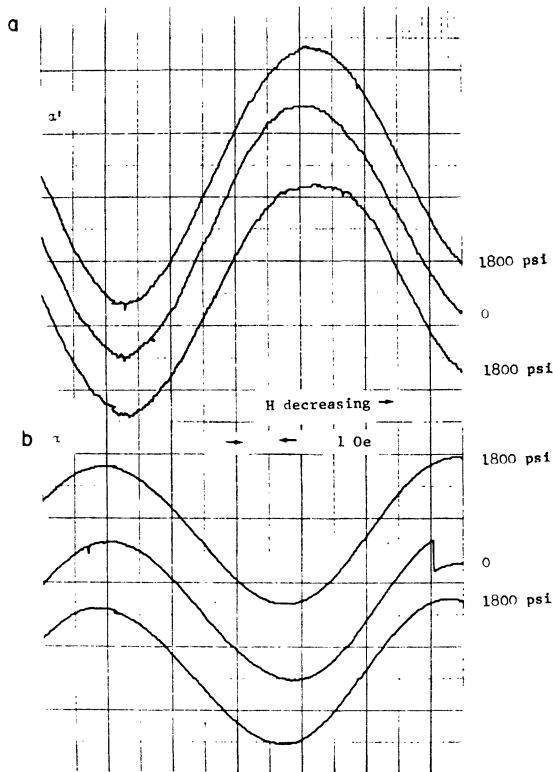


FIG. 5(a). Reproduction of fluid-He phase-shift data of the cigar waist α' frequency for $H||[0001]$. (b) Reproduction of fluid-He phase-shift data of the cigar hip α frequency for $H||[0001]$. Traces were all taken at 4°K and 12.655 kOe.

at the rate of $(2.0 \pm 0.5) \times 10^{-4}$ kbar $^{-1}$, while the cigar waist α' decreases at $-(0.8 \pm 0.4) \times 10^{-4}$ kbar $^{-1}$. These values are weighted averages of the results of determinations of the pressure derivatives by the three methods outlined in Sec. II. The three determinations of both derivatives agreed within the estimated uncertainties. The pressure derivative for the long cross section of the cigar for $H||[11\bar{2}0]$ is $(5.0 \pm 1.5) \times 10^{-4}$ kbar $^{-1}$. This result was obtained by use of the fluid-He phase shift technique, but less accurate results obtained in solid He were consistent with this value.

If Be were free-electron-like, the main effect of hydrostatic pressure would be a scaling of all the cross

TABLE II. Summary of pressure derivatives for cross sections of the third-band electron surface (cigar) of Be. The [0001] frequencies were obtained with *in situ* NMR^a; [11 $\bar{2}0$] values from Ref. 2.

Cross section	Frequency	Field direction	$d \ln F / dP$ (in kbar $^{-1}$)	technique ^b
Cigar hip α	9.72×10^6	[0001]	$2.3 (\pm 0.5) \times 10^{-4}$	method 1
			$1.6 (\pm 0.4) \times 10^{-4}$	method 2
			$2.3 (\pm 0.5) \times 10^{-4}$	method 3
Cigar waist α'	9.43×10^6	[0001]	$-0.7 (\pm 0.5) \times 10^{-4}$	method 1
			$-1.0 (\pm 0.6) \times 10^{-4}$	method 2
			$-0.9 (\pm 0.4) \times 10^{-4}$	method 3
Cigar (2α)	1.06×10^8	[11 $\bar{2}0$]	$5.0 (\pm 1.5) \times 10^{-4}$	fluid He

^a W. J. O'Sullivan and J. E. Schirber, *Cryogenics* **7**, 118 (9167).

^b See text (Sec. II) for detailed descriptions of methods 1, 2, and 3.

TABLE III. Comparison of our pressure derivatives for cross-sectional areas of the Fermi surface of Be with those derivable from the magnetostriction work of Ref. 9, and with the theoretical predictions of Ref. 7. Values of $d \ln F / dP$ given in units of 10^{-4} kbar $^{-1}$.

Cross section	Field Direction	Our result ^a	Magnetostriction result ^b	Theoretical prediction
Coronet waist (γ)	[11 $\bar{2}0$]	-45 ± 10	-160 ± 100	-15 ± 12
	[10 $\bar{1}0$]	...	-50 ± 50	...
Cigar hip (α)	[0001]	2.0 ± 0.5	10 ± 4	1.7 ± 1.0
Cigar waist (α')	[0001]	-0.8 ± 0.4	10 ± 4	-1.9 ± 1.0
Coronet belly (β_1)	[11 $\bar{2}0$]	3 ± 1	...	3.5 ± 1.4

^a Values quoted are a weighted average of the results of the various methods.

^b Error estimated from the quote 20% uncertainty in the strain dependence of the cross-sectional areas.

sections at a rate given by $\frac{2}{3}$ the volume compressibility¹⁷ or 5.8×10^{-4} kbar $^{-1}$. The slight deviation of the Be lattice from close packed ($c/a=1.58$ instead of 1.63) would tend to make the cigars and coronet waists decrease slightly with increasing pressure. It is not particularly useful to compare our pressure results in any quantitative manner with the free-electron-model predictions, because the sizes of the actual cross sections of the Fermi surface of Be differ so radically from the free-electron values. Thus, the magnitude of the shifts predicted depends primarily on the manner in which the model cross sections are scaled to agree with the observed values. In any event, the free-electron model could not account for the simultaneous increase of the cigar hips and decrease in the cigar waists.

A more meaningful comparison can be made with a model such as used by Tripp *et al.*² Their model has been shown to fit the zero-pressure Fermi surface to better than 1%, and in a recent paper Tripp, Everett, Gordon, and Stark⁷ discuss the effect of strain on the Fermi surface of Be. Results of their calculation are shown in Table III. The agreement between the calculated and observed pressure derivatives is well within estimated uncertainties except for coronet waists. In this case, the disagreement is probably not significantly outside the combined calculational and experimental uncertainties.

However, as emphasized by Tripp *et al.*,⁷ the agreement as far as the relative sign of the α and α' cigar pressure derivatives is extremely sensitive to the magnitude of the Fermi energy. A change of only 30 μ Ry would cause the two derivatives to have the same sign. This suggests that in this case, the argument might be reversed, and the experimental information of oppositely signed pressure derivatives for the α and α' cross sections be used to *determine* the Fermi energy.

We are able to compare a portion of our results with the magnetostriction work of Chandrasekhar, Fawcett, Sparlin, and White (CFSW).⁹ They presented data on three cross-sectional areas and their results are also compared with ours in Table III. We have

¹⁷ J. F. Smith and C. L. Arbogast, *J. Appl. Phys.* **31**, 99 (1960).

estimated errors for the pressure derivatives derived from their work from their quoted 20% uncertainty in the strain dependence of the cross-sectional areas. Since our results must be compared with volume rather than strain derivatives, three experimental magnetostriction results must be combined, and the large uncertainties quoted in Table III result from the propagation of error of these individual strain derivatives.

Our result for the pressure derivative of the coronet waists is in satisfactory agreement with the magnetostriction result, but there is essentially no agreement for the cigar cross-section pressure derivatives. The magnetostriction values are nearly an order of magnitude larger, and more significantly are of the same sign for the pressure derivatives of the α and α' sections. We find that the cigar hips increase in size while the cigar waist decreases.

In a preliminary report on these electron surface results,¹⁰ we attributed the disagreement between our directly determined pressure derivatives and those derived from the magnetostriction results to the relatively large errors inherent in the latter method. In our measurements, it is necessary to measure either dHvA frequencies, or changes in frequencies. With the magnetostriction technique, two amplitudes, the magnetostriction and the magnetization, must be determined. It is well known that dHvA-type amplitude measurements, particularly when made on different samples, are difficult to compare in a quantitative manner.

The large anisotropy (4-6 to 1) between the magnetostriction parallel to the c axis and in the basal plane reported by CFSW for the cigar oscillations with $\mathbf{H} \parallel [0001]$ leads to a further, and perhaps more fundamental, disagreement between our data and the magnetostriction results. With this anisotropy, the magnetostriction parallel to the c axis, ϵ_3 , will dominate the volume magnetostriction ϵ . Then with the opposite-signed pressure derivatives $d \ln \alpha / dP$ and $d \ln \alpha' / dP$, the nodes (and antinodes) of the resultant beat pattern of the magnetostriction will not occur at the same fields as do the nodes (and antinodes) of the magnetization pattern.

This is most easily seen by deriving the magnetostriction expressions for two sine waves. We let the subscript 1 denote α and the subscript 2, α' . Neglecting higher harmonics, the Gibbs free energy G is given by

$$G = G_{01} \cos(2\pi F_1/B + \alpha) + G_{02} \cos(2\pi F_2/B + \beta). \quad (7)$$

The *volume* magnetostriction ϵ is given by $\epsilon = -\partial G / \partial P$,

$$\begin{aligned} \epsilon = & \left\{ M_{10} \sin\left(\frac{2\pi F_1}{B} + \alpha\right) \left[B \frac{d \ln F_1}{dP} + \frac{8\pi^2 F_2}{B} M_{20} \cos\left(\frac{2\pi F_2}{B} + \beta\right) \left(\frac{d \ln F_2}{dP} - \frac{d \ln F_1}{dP} \right) \right] \right. \\ & \left. + M_{20} \sin\left(\frac{2\pi F_2}{B} + \beta\right) \left[B \frac{d \ln F_2}{dP} + \frac{8\pi^2 F_1}{B} M_{10} \cos\left(\frac{2\pi F_1}{B} + \alpha\right) \left(\frac{d \ln F_1}{dP} - \frac{d \ln F_2}{dP} \right) \right] \right\} \\ & \times \left[1 - \frac{8\pi^2 F_1}{B^2} M_{10} \cos\left(\frac{2\pi F_1}{B} + \alpha\right) - \frac{8\pi^2 F_2}{B^2} M_{20} \cos\left(\frac{2\pi F_2}{B} + \beta\right) \right]^{-1}. \quad (11) \end{aligned}$$

so that

$$\begin{aligned} \epsilon = & \frac{2\pi F_1}{B} \frac{d \ln F_1}{dP} G_{01} \sin\left(\frac{2\pi F_1}{B} + \alpha\right) \\ & + \frac{2\pi F_2}{B} \frac{d \ln F_2}{dP} G_{02} \sin\left(\frac{2\pi F_2}{B} + \beta\right). \quad (8) \end{aligned}$$

The magnetization M equals $-\partial G / \partial B$, so that

$$\begin{aligned} M = & -\frac{2\pi F_1}{B^2} G_{01} \sin\left(\frac{2\pi F_1}{B} + \alpha\right) \\ & - \frac{2\pi F_2}{B^2} G_{02} \sin\left(\frac{2\pi F_2}{B} + \beta\right) \\ \equiv & -M_{10} \sin\left(\frac{2\pi F_1}{B} + \alpha\right) - M_{20} \sin\left(\frac{2\pi F_2}{B} + \beta\right). \quad (9) \end{aligned}$$

Using the definition in Eq. (9), we can rewrite Eq. (8) as

$$\begin{aligned} \epsilon = & BM_{10} \frac{d \ln F_1}{dP} \sin\left(\frac{2\pi F_1}{B} + \alpha\right) \\ & + BM_{20} \frac{d \ln F_2}{dP} \sin\left(\frac{2\pi F_2}{B} + \beta\right). \quad (10) \end{aligned}$$

By inspection of Eqs. (9) and (10), we see that the oscillatory terms in ϵ will interfere constructively at the same field values as do the oscillatory terms in M , if and only if the two pressure derivatives $d \ln F_1 / dP$ and $d \ln F_2 / dP$ are of the same sign. Particularly at high fields, it is very easy to establish the field position of the nodes and antinodes, and there seems to be no doubt that the ϵ_3 (and therefore with the reported anisotropy ϵ) and M beat patterns *are* in phase. (The abscissa in Fig. 2 in Ref. 9 is incorrect. The position of the antinode at 26 kOe referred to in this reference, however, is correct.)

In view of this inconsistency, it is now apparent why so much emphasis was placed in Sec. II on the determination of the relative sign of the pressure derivatives of the α and α' cross sections. We feel that the experimental results are conclusive, particularly those of method 3, so we are faced with an apparent paradox as far as reconciliation of our results with those obtained from the magnetostriction data of CFSW is concerned.

If in differentiating Eq. (7) to form ϵ , account is taken of $dB/dP = 4\pi dM/dP$ terms, a much more complicated expression for the oscillatory magnetostriction results

We notice that the two extra terms in the denominator are nothing more than $4\pi dM/dB$. When this quantity approaches unity, the wave form of the magnetization is changed radically, and the so-called B - H or magnetic interaction effects are manifested.¹⁸⁻²¹

There are two important differences between Eqs. (10) and (11). First, the amplitude of the oscillatory magnetostriction is enhanced when $4\pi dM/dB$ is near unity. This would affect the magnitude of pressure derivatives obtained from magnetostriction results. Second, the enhancement of the amplitude of the magnetostriction turns out to be largest at field values corresponding to the nodes of the magnetization. Therefore, when the B - H effect dominates, the difference in sign of the two pressure derivatives is necessary for the beat pattern of ϵ to be in phase with the beat pattern of M .

There are, however, several important objections to this approach:

(1) The B - H terms in Eq. (11) are eliminated by a more realistic choice of Gibbs free energy. Using, as suggested by Pippard¹⁹ (and Holstein), $G = A_{LK}(B) + 2\pi M^2$ (where A_{LK} is the Lifshitz-Kosevich expression²² for the oscillatory thermodynamic potential), the interaction terms in Eq. (11) vanish identically.

(2) If Eq. (11) were valid, we could expect that at sufficiently low fields and/or high temperatures, the interaction terms would become negligible. The beat patterns of M and ϵ_3 would then be out of phase. This behavior has *not* been observed.

(3) Very recent work by Testardi and Condon²³ on the oscillatory velocity of sound in Be indicates that the hexagonal axis/basal plane anisotropy of the strain derivatives of α and α' cross sections is considerably less than found by CFSW. This technique gives only the square of the strain derivatives, but assuming the same signs observed by CFSW, their results lead to values of $d \ln \alpha / dP$ and $d \ln \alpha' / dP$ not inconsistent with ours.

(4) The theoretical description given by Tripp *et al.*⁷ is consistent with both our pressure derivatives, and in phase magnetostriction and magnetization patterns. This occurs because the anisotropy of the calculated strain derivatives along the hexagonal axis to those in the basal plane is less than two. (This latter statement

assumes the two strain derivatives in the basal plane are essentially equal.)

The above considerations lead us to believe that the magnetostriction anisotropy is probably considerably smaller than that reported in Ref. 9. The apparent paradox of identical node and antinode positions in the magnetostriction and magnetization with our pressure derivatives does not then arise, and it is not necessary to invoke an analysis such as Eq. (11) to reconcile the two types of data.

IV. SUMMARY AND CONCLUSIONS

We have measured the effect of hydrostatic pressure on cross sections for major symmetry directions of both the second-zone hole sheet and the third-zone electron sheets of the Fermi surface of Be. Measurements of several of the cross sections as determined from dHvA frequencies were made in both solid He to ~ 4 kbar, and in fluid He. The results of the two types of pressure measurement are in excellent agreement in all cases.

The change of the cross-sectional areas with pressure differs substantially from what the free-electron model would predict, but this is not surprising in that the cross sections themselves are much different in size than those given by the model.

A comparison of our data with the results of the nonlocal pseudopotential model of Tripp *et al.*⁷ shows quite satisfactory agreement. We can compare a portion of our results with pressure derivatives derivable from the oscillatory magnetostriction work of CFSW.⁹ The results are in satisfactory agreement for the waists of the second-zone coronet, but show disagreements with respect to both sign and magnitude for the third-zone cigar cross sections for $H_{||}[0001]$. The difference in sign of the two cigar cross-section pressure derivatives has been demonstrated rather conclusively by new data presented in this paper. This sign difference leads to an apparent paradox involving the relative positions in field of nodes and antinodes in the magnetostriction and magnetization. This "paradox" depends critically on the hexagonal axis/basal plane anisotropy of the magnetostriction. We conclude that the anisotropy in the magnetostriction is probably considerably less than reported, so that it is likely that no paradox arises.

ACKNOWLEDGMENTS

We wish to thank L. E. Brubaker for his technical assistance. We are indebted to Dr. W. L. Gordon for the loan of his Be crystals and to Dr. G. London for the gift of a Be sample. We acknowledge stimulating discussions with Dr. D. M. Sparlin and thank Dr. J. H. Tripp, Dr. P. M. Everett, Dr. W. L. Gordon, and Dr. R. W. Stark in addition to Dr. L. R. Testardi and Dr. J. H. Condon for access to their work before publication.

¹⁸ J. H. Condon, Phys. Rev. **145**, 526 (1966).

¹⁹ A. B. Pippard, Proc. Roy. Soc. (London) **A272**, 192 (1963).

²⁰ D. Shoenberg and J. J. Vuillemin, in *Proceedings of the Tenth International Conference on Low Temperature Physics, Moscow, 1966*, edited by M. P. Malkov (Proizvodstrenno-Izdatesk'ii, VINITI, Moscow, 1967).

²¹ D. Shoenberg, Can. J. Phys. **46**, 1915 (1968); D. Shoenberg and I. M. Templeton, *ibid.* **46**, 1925 (1968).

²² I. M. Lifshitz and A. M. Kosevich, Zh. Eksperim. i Teor. Fiz. **29**, 730 (1955) [English Transl.: Soviet Phys.—JETP **2**, 635 (1956)].

²³ L. R. Testardi and J. H. Condon, Bull. Am. Phys. Soc. **14**, 400 (1969); and private communication.

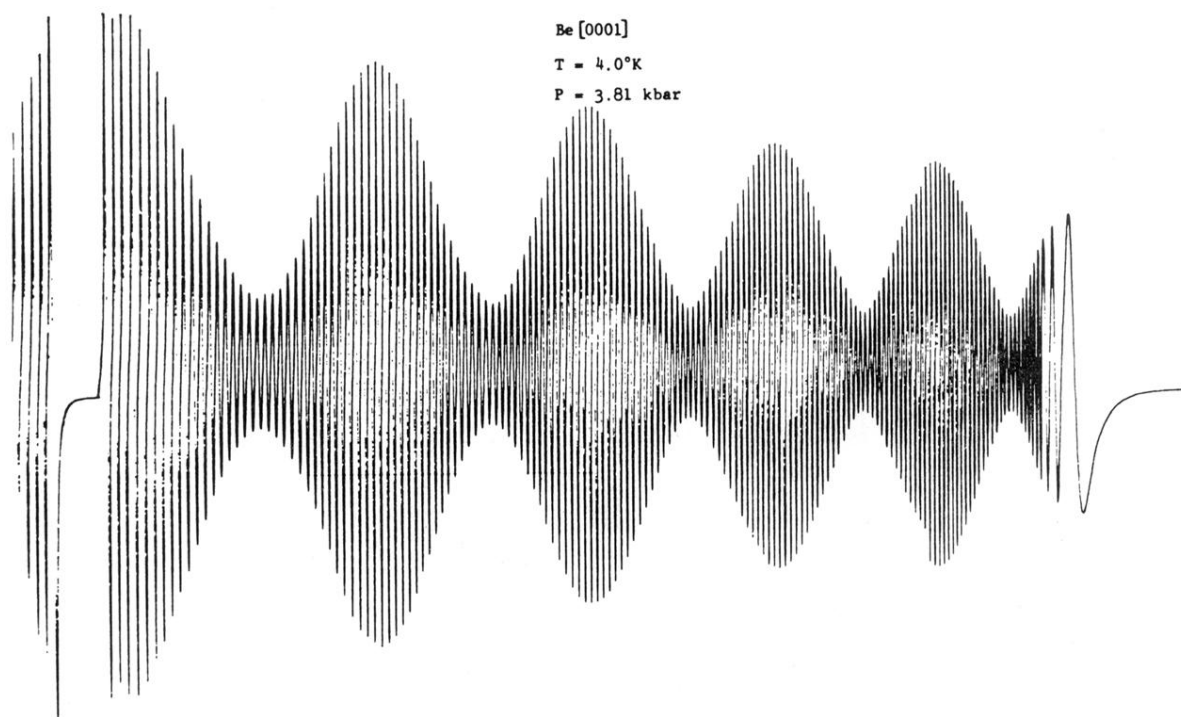


FIG. 2. Reproduction of the third-zone electron (cigar) oscillations in the magnetization for $H \parallel [0001]$.